

This article was downloaded by:

On: 25 January 2011

Access details: *Access Details: Free Access*

Publisher *Taylor & Francis*

Informa Ltd Registered in England and Wales Registered Number: 1072954 Registered office: Mortimer House, 37-41 Mortimer Street, London W1T 3JH, UK



Liquid Crystals

Publication details, including instructions for authors and subscription information:

<http://www.informaworld.com/smpp/title~content=t713926090>

On the origin of high optical director tilt in a partially fluorinated orthoconic antiferroelectric liquid crystal mixture

Jan P. F. Lagerwall Corresponding author^a; Alexander Saipa^a; Frank Giesselmann^a; Roman Dabrowski^b

^a Institute of Physical Chemistry, University of Stuttgart, D-705 69 Stuttgart, Germany ^b Military University of Technology, 00-908 Warsaw, Poland

Online publication date: 21 May 2010

To cite this Article Lagerwall Corresponding author, Jan P. F. , Saipa, Alexander , Giesselmann, Frank and Dabrowski, Roman(2004) 'On the origin of high optical director tilt in a partially fluorinated orthoconic antiferroelectric liquid crystal mixture', *Liquid Crystals*, 31: 9, 1175 – 1184

To link to this Article: DOI: 10.1080/02678290410001732279

URL: <http://dx.doi.org/10.1080/02678290410001732279>

PLEASE SCROLL DOWN FOR ARTICLE

Full terms and conditions of use: <http://www.informaworld.com/terms-and-conditions-of-access.pdf>

This article may be used for research, teaching and private study purposes. Any substantial or systematic reproduction, re-distribution, re-selling, loan or sub-licensing, systematic supply or distribution in any form to anyone is expressly forbidden.

The publisher does not give any warranty express or implied or make any representation that the contents will be complete or accurate or up to date. The accuracy of any instructions, formulae and drug doses should be independently verified with primary sources. The publisher shall not be liable for any loss, actions, claims, proceedings, demand or costs or damages whatsoever or howsoever caused arising directly or indirectly in connection with or arising out of the use of this material.

On the origin of high optical director tilt in a partially fluorinated orthoconic antiferroelectric liquid crystal mixture

JAN P. F. LAGERWALL*, ALEXANDER SAIPA, FRANK GIESSELMANN

Institute of Physical Chemistry, University of Stuttgart, Pfaffenwaldring 55,
D-705 69 Stuttgart, Germany

and ROMAN DABROWSKI

Military University of Technology, 00-908 Warsaw, Poland

(Received 31 March 2004; accepted 15 April 2004)

We have investigated the orthoconic antiferroelectric liquid crystal mixture W107 by means of optical, X-ray and calorimetry measurements in order to assess the origin of the unusually high tilt angle between the optic axis and the smectic layer normal in this material. The optical birefringence increases strongly below the transition to the tilted phases, showing that the onset of tilt is coupled with a considerable increase in orientational order. The layer spacing in the smectic A* (SmA*) phase is notably smaller than the extended length of the molecules constituting the mixture, and the shrinkage in smectic C* (SmC*) and smectic C_a* (SmC_a*) is much less than the optical tilt angle would predict. These observations indicate that the tilting transition in W107 to a large extent follows the asymmetric de Vries diffuse cone model. The molecules are on average considerably tilted with respect to the layer normal already in the SmA* phase but the tilting directions are there randomly distributed, giving the phase its uniaxial characteristics. At the transition to the SmC* phase, the distribution is biased such that the molecular tilt already present in SmA* now gives a contribution to the macroscopic tilt angle. In addition, there is a certain increase of the average tilt angle, leading to a slightly smaller layer thickness in the tilted phases. Analysis of the wide angle scattering data show that the molecular tilt in SmC_a* is about 20° larger than in SmA*. The large optical tilt (45°) in the SmC_a* phase thus results from a combination of an increased average molecule tilt and a biasing of tilt direction fluctuations.

1. Introduction

Antiferroelectric liquid crystals (AFLCs) soon after their discovery, were pointed out as most interesting candidates for active materials in future display devices [1]. As with ferroelectric liquid crystals (FLCs) they promise displays with high speed operation, in-plane switching and ultra-high resolution. In addition, they have the advantages that true grey scale can easily be achieved and that the driving is intrinsically d.c.-compensated. A major problem was however encountered at an early stage in the difficulty to align AFLC materials. Much work has been devoted to solving this problem but some years ago the industrial development of AFLC displays came to a halt.

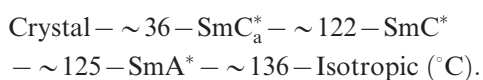
A possible way around the problem was proposed and demonstrated by D'havé *et al.* [2–4]. Since the main adverse effect of bad alignment is light leakage in the dark

state of the device, leading to a strong reduction in contrast, it is the dark state that has to be improved. The suggested solution is based on the fact that if the optical director of each layer of a surface-stabilized (non-helical) SmC_a* phase is tilted at 45° with respect to the layer normal, **k**, in the anticlinic state (i.e. with the tilt direction reversing from layer to layer) the cell becomes optically uniaxial with its optic axis perpendicular to the cell plane. This means that the smectic layers can be aligned in any direction in the plane of the cell, and the cell will still look perfectly black between crossed polarizers. Therefore, a device built with such *orthoconic* (the name derived from the opening angle of the smectic tilt cone being 90°) antiferroelectric liquid crystals has a perfect dark state regardless of the uniformity of the alignment. By using orthoconic AFLCs, or OAFLCs, it may thus be possible to produce an AFLC display of very high quality. Because of this realization, there has been a considerable interest in developing new OAFLC materials that can be used in display devices.

*Author for correspondence;
e-mail: jan.lagerwall@ipc.uni-stuttgart.de

In this paper we report the investigation of the origin of the very high optical director tilt θ_{opt} , in an OAFLC mixture. A naïve picture, which nevertheless is quite widespread, is that the magnitude of the optical tilt is the same as the angle between the molecular long axis and \mathbf{k} . The real situation is not so simple. First of all, one must consider the thermal orientational disorder, which means that the molecules can tilt both more and less than the optical tilt angle. This difference is particularly obvious in the SmA* phase, where $\theta_{\text{opt}}=0$ but where the average molecular tilt resulting from the orientational fluctuations is typically of the order of 20° [5]. Furthermore, experiments where the optical tilt angle has been compared with the ‘steric tilt angle’ obtained by X-ray measurements generally show that θ_{opt} can be considerably larger than the X-ray tilt [6–8]. Finally, the optical director tilt angle is not even a uniquely defined variable, because its magnitude in tilted smectics is dependent on the wavelength at which the tilt angle is measured, shorter wavelengths producing larger θ_{opt} values [9]. The origin of the optical tilt is thus a fundamentally intriguing issue, but with the new interest in finding high tilt AFLC materials it has also become technologically very important.

We have investigated one of the first OAFLC mixtures, W107, by means of various optical, electro-optical and X-ray methods. This mixture is particularly interesting because it exhibits both the orthogonal SmA* phase and the two tilted phases SmC* and SmC_a*, yet it suffers surprisingly few problems with textural defects, something which is otherwise often connected with the transition between an orthogonal and a tilted phase. Considering that the tilt is extremely high in the case of W107, this is indeed puzzling. The phase sequence of W107 is:



The transition temperatures indicated should be regarded only as guidelines; W107 is a four component mixture and all phase transitions are first order, hence supercooling effects and phase coexistence are unavoidable characteristics of the material, making the definition of distinct transition temperatures impossible. Furthermore, the many components of the mixture render it very difficult to create two identical batches. This became apparent during our study, when two different batches were used for early and late experiments. A large sensitivity to the mixture composition was observed in the temperature of the SmC*–SmC_a* transition which in batch 1 was some 7 K lower than in batch 2, thus extending the synclinal temperature range by about the same amount. Differences between the batches in other parameters were negligible.

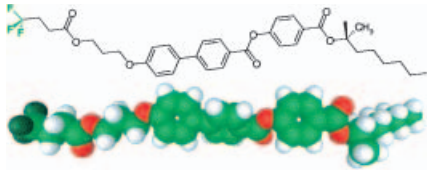
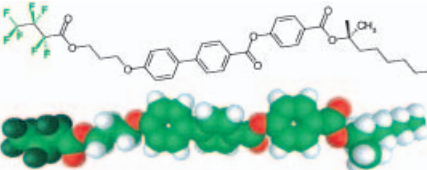
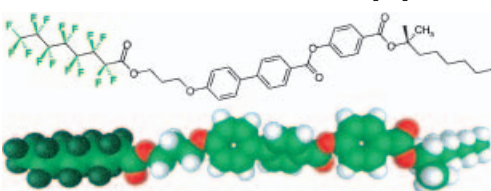
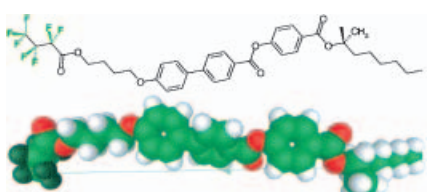
The four components of the mixture are pictured in the table, together with their respective phase sequences, saturated optical tilt and spontaneous polarization, \mathbf{P}_s . Note that all components have a partially fluorinated achiral terminal chain. The different components actually differ only in the constitution of this chain, the mesogenic core and the chiral terminal chain being identical in all four constituent structures.

2. Experimental

For X-ray investigations the material was filled into Mark capillary tubes of 0.7 mm diameter, and for the optical microscopy studies we used polyimide-coated planar-aligning cells with 2 μm cell gap. All optical studies were carried out with the sample placed in an Instec MK1 hot stage fitted to an Olympus BH-2 polarizing microscope. The light was monochromatized using interference filters and the transmission was measured using a photo diode (FLC Electronics). For determining the optical tilt θ_{opt} , the optical transmission (T) of the \mathbf{P}_s up and down states, obtained through saturated square wave switching, was measured for several consecutive sample orientations φ . By fitting two \sin^2 functions to the two resulting $T(\varphi)$ data sets very precise values of θ_{opt} can be extracted [9]. The high resolution measurements of θ_{opt} and the birefringence Δn were performed using a temperature scanning technique described in detail by Saipa and Giebelmann [15]. In brief, the method is based on monitoring the sample temperature and optical transmission while slowly heating or cooling the sample through the mesophases at constant rate. The scan is repeated in four different measuring geometries: crossed and parallel polarizers and, for each case, layer normal \mathbf{k} parallel and at 45° angle to the polarizer direction p . With these four data sets, the transmittances between crossed polarizers when the sample is oriented with \mathbf{k} parallel to p , τ_1 , or at 45° to p , τ_2 , can be calculated. Since θ is a function of the quotient τ_1/τ_2 , and Δn a function of the sum $\tau_1+\tau_2$, these parameters can now be extracted. Data were collected during switching with a 55.1 Hz square wave.

The spontaneous polarization was measured by the triangular wave polarization reversal method [16]. The transition enthalpies and temperatures were determined using a Perkin Elmer DSC 7 calorimeter on cooling and on heating at 5 K min^{-1} . For the X-ray measurements, a CuK_α radiation source was used. Small angle scattering data from unaligned (powderlike) samples were obtained using a Kratky compact camera (A. Paar) and a one-dimensional electronic detector (M. Braun), giving a measure of the smectic layer spacing d with a resolution better than 0.1 \AA in the range of interest. In order to measure the molecular orientational distribution, we used an imaging plate system (Fuji BAS SR) for recording the

Table. The orthoconic AFLC mixture W107 and its components.

Component	Amount in mixture/%	Chemical constitution (space filling model minimized by MOPAC) and phase sequence	All-trans length/Å	$d_{\max} \rightarrow d_{\min}/$ Å	θ_{opt} (saturated)/degrees	P_s (saturated)/nC cm ⁻²
1	6.31	 Cr – 99 – SmC _a * – 111.3 – SmC* – 122.2 – SmA* – 126.8 – I [10]	35.0	35.0 ↓ 33.0[10]	31[10]	175[10]
2	20.77	 Cr – 83.5 – (SmI _a * – 54 –) SmC _a * – 121 – SmC* – 123.6 – SmA* – 128.8 – I [10]	35.6	33.2 ↓ 30.0[10]	34[11]	340[10]
3	32.45	 Cr – 68.8 – SmC _a * – 100.7 – SmC* – 129.7 – SmA* – 153.2 – I [12]	41.0	37.0 ↓ 34.1[13]	35.5[13]	> 75[14]
4	40.47	 Cr – 69.8 – SmC _a * – 120.7 – SmC* – 125.6 – I [10]	35.1	30.5 ↓ 29.5[10]	40.3[10]	200[10]

two-dimensional wide angle scattering (WAXS) pattern from samples aligned by a magnetic field (1 T). The scattering patterns were analysed using a technique described in detail in a previous paper [7]. Levelut and co-workers proposed a very useful expansion for the wide angle scattering intensity profile, i.e. the intensity I as a function of scattering direction χ :

$$I(\chi) = \sum_{n=0}^{\infty} f_{2n} \frac{2^n n!}{(2n+1)!!} \cos^{2n} \chi. \quad (1)$$

We fitted this expansion to the scattering data obtained in the SmA* phase. If the average molecular tilt increases, as is expected in the SmC* and SmC_a* phases as compared with

SmA*, the wide angle scattering pattern maximum broadens. If we neglect the difference in orientational order between the SmA* phase and the tilted phases, we can use the SmA*-fitted expansion as a template and fit the scattering data of the tilted phases with a pair of SmA* expansions, shifted away from $\chi=0$ by the same amount but in different directions. The magnitude of the shift necessary to obtain a good fit gives an estimate of how much the average molecule tilt has increased in the tilted phases.

3. Results

3.1. Optical and electro-optical investigations

The values of P_s and θ_{opt} of W107 are shown in figure 1 as a function of temperature. In the right-hand diagram the tilt angles for two temperatures at which

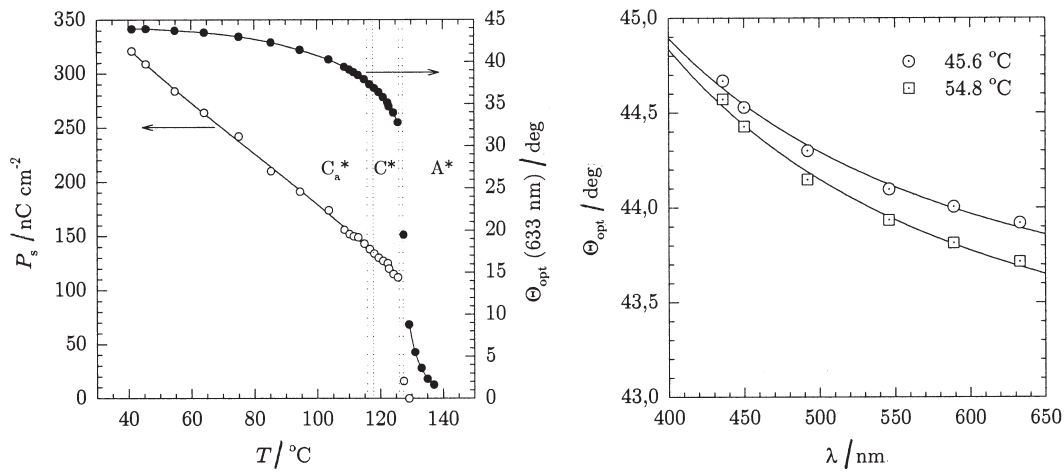


Figure 1. Left diagram: spontaneous polarization P_s (empty circles) and optical tilt angle θ_{opt} at 633 nm (filled circles) of W107 (batch 1) as a function of temperature. Right diagram: θ_{opt} at two temperatures in the SmC_a^* phase as a function of wavelength λ (batch 1).

the mixture is in the SmC_a^* phase are shown as a function of measuring wavelength. As is usually the case in tilted smectics [9], θ_{opt} increases with decreasing wavelength. Close to room temperature the tilt measured with blue light approaches 45° , whereas the angle measured with red light saturates at about 44° . The dispersion is thus about 2%, which is quite small (5–10% dispersion was measured with standard FLCs by Giesselmann *et al.* [9]). A curiosity of the spontaneous polarization is that it shows no sign of saturating as the temperature is decreased. Such a behaviour has been reported previously for some ferroelectric liquid crystals [17–19] but the perfectly linear increase exhibited throughout the temperature range of SmC^* and SmC_a^* in W107 is quite exceptional.

Component 2 on its own behaves similarly [11]. The behaviour indicates strong biquadratic polarization – tilt coupling [20, 21], the effect of which will be particularly strong in high tilt materials such as W107.

Not only the $\text{SmC}^* - \text{SmC}_a^*$ transition but also the tilting transition is first order, as is easily recognized by the step-like discontinuities in the left-hand diagram of figure 1, both in P_s and in θ_{opt} . In figure 2 the DSC thermogram for W107 is given next to a high resolution plot of the optical transmission between crossed polarizers of a $2\ \mu\text{m}$ thick planar-aligned sample, as it is heated at constant rate from SmC_a^* to SmA^* under the influence of a weak a.c. electric field. The transition enthalpy of the $\text{SmC}^* - \text{SmC}_a^*$ transition is quite small, in particular in comparison with the $\text{SmA}^* - \text{SmC}^*$

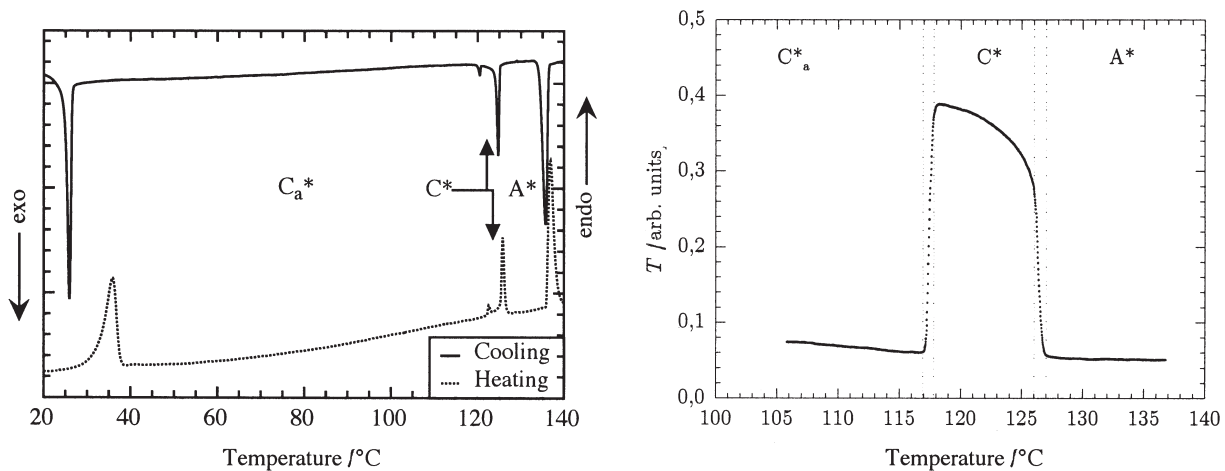


Figure 2. Two ways of distinguishing the first order $\text{SmA}^* - \text{SmC}^*$ and $\text{SmC}^* - \text{SmC}_a^*$ transitions. To the left is the DSC thermogram (batch 2) and to the right the optical transmission between crossed polarizers of a $2\ \mu\text{m}$ cell, aligned such that the smectic layer normal \mathbf{k} is parallel to the polarizer, on heating from SmC_a^* to SmA^* (batch 1).

transition. But in the optical transmission vs. temperature diagram the transition between syn- and anticlinic behaviour is made clearly visible. In this plot the biphasic regions surrounding the SmC^* phase are also easy to recognize. The sample was slowly heated during the experiment (0.2 K min^{-1}), so had the sample been a pure compound the transmission should have changed clearly step-wise at the $\text{SmC}_a^*-\text{SmC}^*$ and $\text{SmC}^*-\text{SmA}^*$ transitions. But since we are studying a mixture, both these first order transitions allow for a considerable phase coexistence resulting in the transmission curve looking almost continuous across the transitions.

In figure 3 the birefringence Δn as a function of temperature is shown. The data were obtained by switching the sample with a square wave during heating at a constant speed, with a voltage level assuring that all measurements were taken in the synclinic state. The large increase in Δn in SmC^* and SmC_a^* as compared with SmA^* is a strong indication that the SmA^* phase is considerably more disordered than the tilted phases in their non-helical synclinic states. This suggests that the tilting transition to a large extent follows the *asymmetric diffuse cone model* (in the following referred to as the ADC model) of Adrian de Vries [5, 22–24], in which the generation of macroscopic optical tilt is attributed to the biasing of a distribution of tilted molecules (the distribution is uniform in SmA^*). We have previously studied other chiral smectics with one terminal chain partially fluorinated, in that case the chain containing the stereogenic centre, and we could show that those compounds are almost perfect examples of FLCs and AFLCs exhibiting a tilting transition according to de Vries' model [7, 8]. It is therefore not so surprising that W107, the components of which are all partially fluorinated, also exhibits a tilting transition close to the ADC model. The increase in Δn between SmA^* and the fully switched SmC_a^* phase in W107 is about 52%, thus even much more

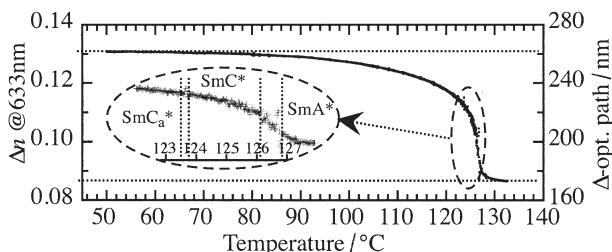


Figure 3. The birefringence Δn of W107 (batch 2) measured as a function of temperature at a wavelength of 633 nm. The right-hand y -axis shows the resulting optical path difference for this particular planar-aligned $2 \mu\text{m}$ cell. The inset shows a magnification of the behavior in the transitional region.

drastic than in the other fluorinated asymmetric diffuse cone model materials. In the FLC compound the difference was about 14% and in the corresponding AFLC mixture it was roughly 27%.

3.2. X-ray diffraction investigations

The smectic layer thickness d obtained by small angle X-ray scattering (SAXS) experiments is plotted as a function of temperature in figure 4. In the same diagram the expected layer spacing behaviour for a hypothetical rigid-rod molecule system where the optical tilt angle actually reflects the molecular tilt according to $d_C = d_A \cos \theta_{\text{opt}}$ is plotted. It is quite obvious from this comparison that, although the smectic layers do shrink at the onset of tilt, the magnitude of the shrinkage is nowhere near what the optical tilt angle would suggest. Furthermore, the maximum layer spacing, measured in the SmA^* phase, is about 33 \AA . This is smaller than the extended length of each of the four components, the difference being as much as 8 \AA ($\sim 25\%$) in the case of component 3. It is also interesting to look at the actual SAXS profiles as a function of temperature, shown in the left-hand part of the figure. What is striking is how the scattering intensity drastically increases below the onset of tilt, in particular in the anticlinic SmC_a^* phase. This change shows that the translational order (smectic order) is much higher in SmC_a^* than in SmA^* and to some extent than in SmC^* . This can be understood by considering that the absence of a uniform tilting direction in SmA^* gives this phase considerable freedom in how the layers are formed. Molecules can quite easily interdigitate, i.e. partially move into the neighbouring layers. Although this is a characteristic also of the SmC^* phase, the anticlinic structure of SmC_a^* makes this much more difficult [25–27]. Furthermore, the distribution in the molecular tilt present in any orientationally disordered SmA^* phase may give this phase undulated smectic layers, a structure which is not compatible with the more uniform molecule tilt present in SmC^* and SmC_a^* . The reduced degrees of freedom in SmC^* and, in particular, SmC_a^* can thus be expected to increase the degree of translational order along \mathbf{k} , explaining the increased scattering intensity.

In figure 5, two-dimensional wide angle X-ray scattering (WAXS) patterns from an aligned sample are shown together with best fits of equation (1) to the scattering data. The higher degree of order in SmC_a^* is here reflected in the larger number of harmonics corresponding to the smectic layer periodicity. Whereas only the fundamental can be detected in the SmA^* phase, it is easy to observe harmonics up to fourth order in the SmC_a^* pattern. Interestingly, the strongest

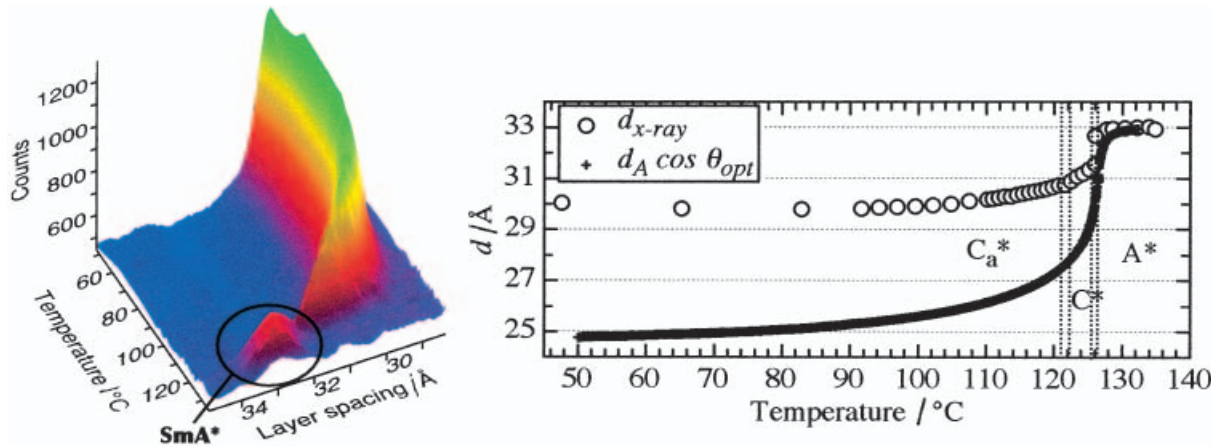


Figure 4. The small angle X-ray scattering profile of W107 (batch 2) as a function of temperature (left) together with the smectic layer spacing d extracted from these data (right diagram, circles). The layer spacing data are plotted together with the behavior which would have resulted if the optical tilt angle at all temperatures had reflected an increased average molecular tilt (rhombohedra).

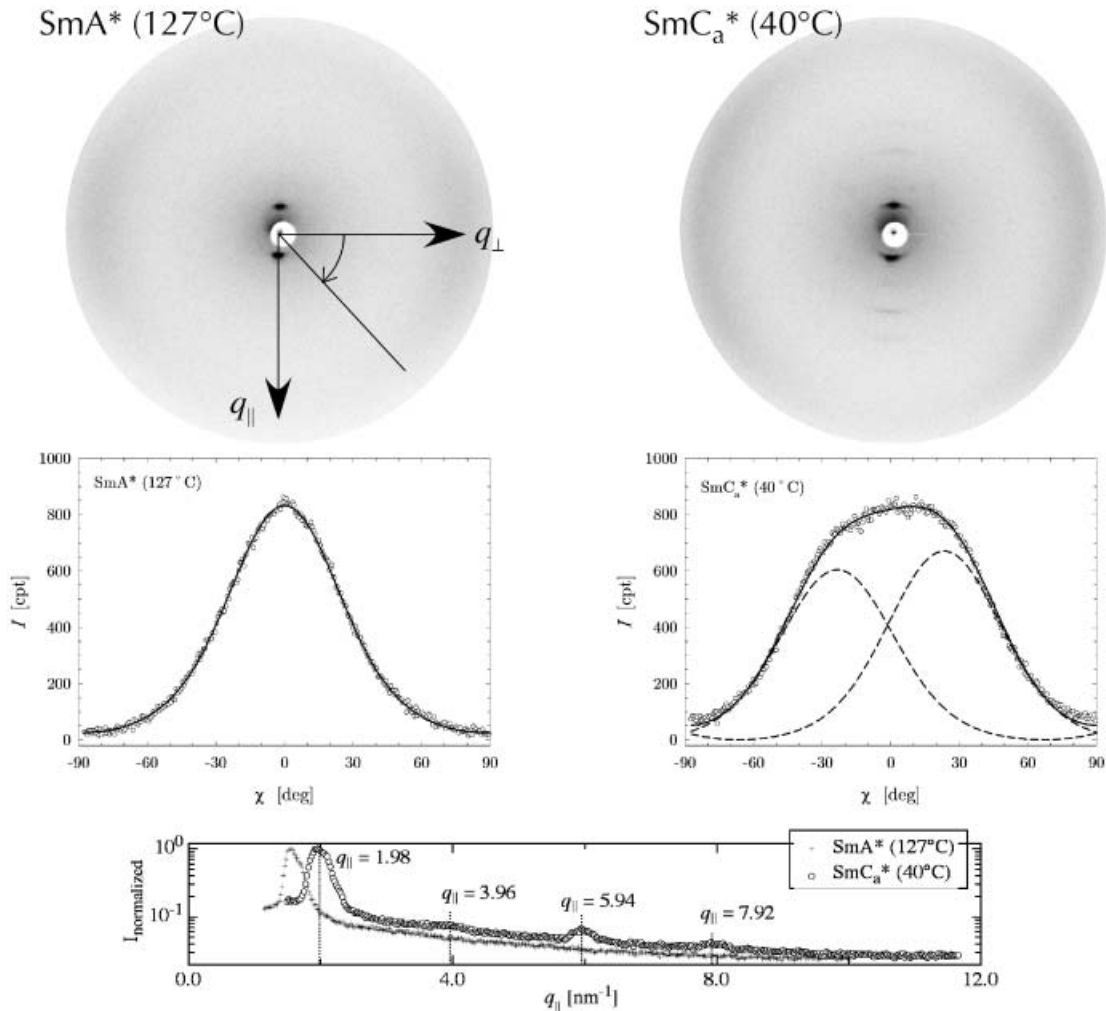


Figure 5. Top row: X-ray scattering patterns from an aligned sample of W107 (batch 2) in the SmA^* and SmC_a^* phases. Middle: the wide angle scattering intensity as function of scattering direction χ , together with best fits of equation (1) to the data. Bottom: the integrated scattering intensity as a function of diffraction angle q_{\parallel} . Note the higher harmonics to the layer diffraction peak present in the SmC_a^* phase, but absent in SmA^* .

harmonic is the third, whereas the second and fourth are quite weak. This shows that the electron density wave along \mathbf{k} in this system significantly deviates from a plain sinusoidal modulation. This is most likely a result of the heavily fluorinated tails, leading to electron density maxima outside the mesogen core. The diffuse scattering in the wide angle regime reflects the intermolecular spacing within the layers, i.e. the lateral molecular spacing. In both phases this scattering has its maximum intensity at 90° to the smectic layer pseudo-Bragg peaks, as expected for a SmA^* phase and a helical SmC_a^* phase. In the tilted phase the maximum is broader, reflecting a larger average molecule tilt. With the incorrect but simplifying assumption that the orientational order around the local director in SmA^* and SmC_a^* are the same we can fit (see §2) the broader SmC_a^* peak with two copies of the fitted SmA^* function, shifted by the same angle but in opposite directions; in that way we obtain an estimate of the increase of average molecular tilt in SmC_a^* as compared with SmA^* , a quantity we denote as θ_{WAXS} .

We are now in a position to compare three different experimental measures of tilting in W107: the optical tilt angle, the SAXS tilt angle corresponding to the decrease in layer spacing, and the WAXS tilt angle corresponding to the broadening of the maximum in the diffuse wide angle scattering. This comparison is shown in figure 6. It is noteworthy that the two X-ray tilt angles resemble each other quite well, whereas the optical tilt angle is about 70–100% larger than the other two at low temperatures.

4. Discussion

4.1. Comparison between the mixture and its separate components

In relation to the analysis of the W107 mixture it is interesting first to look at the properties of the four components alone. Comparing components 1 and 2 we

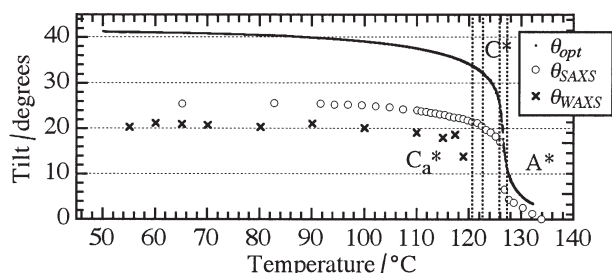


Figure 6. Three different measures of tilt angle in W107 (batch 2): the optical director tilt angle, the SAXS tilt angle extracted from the layer shrinkage, and the increased average molecule tilt with respect to the SmA^* situation extracted from the WAXS patterns, as a function of temperature.

first notice that the change from $\text{C}_2\text{H}_4\text{CF}_3$ to C_3F_7 at the end of the achiral terminal chain leads to a doubling of \mathbf{P}_s . This is remarkable because the structural change has only a small influence on the transverse molecular dipole moment and the chiral sides of the molecules are identical. The optical tilt angle is slightly larger for component 2, but the difference is much too small to explain the \mathbf{P}_s doubling. The explanation for the difference must lie in the collective behaviour of the molecules, which must thus be influenced by the addition of fluorine substituents to the achiral end chain. For example, the two structures may pack in different manners within the smectic layers, such that a larger effective polarization arises through an enhanced biasing of molecular rotations with component 2 [28].

As for the phase sequence, we note that these two components exhibit the same types of smectic phases and that the clearing points and temperatures of onset of tilt are essentially identical. On the other hand, the temperature range of the SmC_a^* phase is much larger, at the cost of the SmC^* phase, in the more fluorinated compound, a situation which may well have its origin in the large polarization. However, on adding four difluoromethylene groups to the structure of component 2, i.e. going to component 3, it is the SmC^* phase that broadens at the cost of the anticlinic phase. This component, which is considerably longer than the other three, furthermore has a much higher clearing point and a relatively broad SmA^* phase. The latter phase is narrow in components 1 and 2 (about 5 K), and absent in component 4. Component 4 is structurally similar to component 2, but the additional methylene group in the spacer between mesogenic core and fluorinated terminal moiety affects the geometry of the molecule such that the achiral chain exhibits a distinct kink, whereas the achiral chain in the other three components is more or less straight (the conformations shown are results of MOPAC/AM1 energy minimizations). The kink at the end of the molecule may make it more difficult for the molecules to interdigitate between layers, hence the smectic order is increased and thus a tilted phase, in particular with anticlinic arrangement, is promoted. As expected below a direct isotropic– SmC^* transition, the tilt angle is relatively large, but the polarization is actually distinctly lower than in the related component 2. The temperature of the syn- to anti-clinic transition is almost identical in components 2 and 4.

When the four components are mixed together as W107 the SmC_a^* temperature range is extended towards lower temperatures, whereas the transition between syn- and anticlinic order remains at about the same temperature as in components 2 and 4. The temperature of onset of tilt is unaffected by the mixing and is close to an average value of the tilt onset temperatures

of the components, varying between 122° and 129°C. The larger maximum optical tilt of the mixture, as compared with the single components, can thus to some extent be attributed to an extended temperature range of tilted smectic order.

Components 2 and 3 both exhibit SmA* d -values that are distinctly smaller than the respective molecule length L , showing that the molecules are tilted already in SmA*, in agreement with the diffuse cone model. Component 4, which has no SmA* phase, exhibits layer spacings in SmC* and SmC_a* corresponding to a molecular tilt (calculated according to $d = L \cos \theta_{\text{mol}}$) of 30°–33°, i.e. considerably less than $\theta_{\text{opt}} \approx 40^\circ$. The same holds for component 1 which has a minimum SmC_a* d -value corresponding to a 20° molecule tilt, more than 10° smaller than θ_{opt} . These discrepancies suggest that the ‘rods’ building the smectic layers are actually longer than L , e.g. being built up of bimolecular aggregates. This phenomenon, of which we have found strong indications also in other fluorinated smectics [7, 8], could then also reconcile the SmA* layer spacing of component 1 with the diffuse cone model: if the ‘rods’ were single molecules we would have to have perfect orientational order to get the measured $d \approx L$.

When comparing the layer spacing data of the pure components with those of the mixture it is somewhat surprising that the mixture d -values are similar to those of components 2 and 4. Considering that one third of the mixture consists of component 3, which has a considerably larger molecule length and in the pure state builds smectic phases with notably thicker layers, one would have expected an increase in d . Instead, the layer spacing of the mixture is very similar to that of component 2, both regarding the limiting values and the sudden drop at the SmA*–SmC* transition. This may be another origin of the large optical tilt value obtained in W107: one third of the molecules are inclined more than they would normally have been because they are squeezed into a layer structure in which they do not really fit. A curiosity of component 2 that the mixture does not share is that the sudden drop in d at the SmA*–SmC* transition is not connected to a discontinuous jump in θ_{opt} or in \mathbf{P}_s [10]. These parameters rise quite continuously from zero as the temperature is lowered from SmA* to SmC*, but then jump discontinuously at the SmC*–SmC_a* transition. In other words, the jumps in ‘X-ray tilt’ and θ_{opt} occur at different temperatures, corresponding to different phase transitions. The transition enthalpies reflect the behaviour of the layer spacing, with a SmA*–SmC* enthalpy of 1.2 kJ mol^{−1} and a SmC*–SmC_a* enthalpy of 0.08 kJ mol^{−1}. In the mixture, θ_{opt} , d and \mathbf{P}_s all exhibit their discontinuities at the SmA*–SmC*

transition, which also has a much larger transition enthalpy than the SmC*–SmC_a* transition.

4.2. The nature of the smectic A* phase and the origin of the large optical tilt in SmC* and SmC_a*

There are two strong indications of a major difference in the molecular ordering between the SmA* and the SmC*/C_a* phases. First, we observe much stronger X-ray scattering intensity, and a corresponding enhancement of higher order diffraction maxima, in the tilted phases. The second sign is the considerable increase in optical birefringence observed as the sample is cooled from SmA* to SmC* and SmC_a*. The X-ray results signify that the tilted phases exhibit higher translational order than the SmA* phase, and the optical results show that the orientational order is also higher. The latter observation is a typical ‘fingerprint’ of the de Vries ADC model tilting transition. According to this model the molecules are on the average strongly tilted with respect to \mathbf{k} in the SmA* phase. The SmA*–SmC* transition, i.e. the appearance of macroscopic optical tilt, is mainly a result of ordering of tilting directions on large time- and length-scales. Such a tilting transition induces a macroscopic tilt without affecting the layer spacing, but the increased orientational order is reflected by an increased birefringence. The ADC, the tilted diffuse cone (TDC) and the combined (TADC) models for the SmA–SmC transition are schematically illustrated in figure 7 (for picture clarity reasons the cone is drawn sharp, not diffuse, and the molecule distribution is drawn regular).

Since there is layer shrinkage at the SmA*–SmC* transition of W107, the tilting in this mixture is however clearly not due to biasing of tilting directions alone. The high optical tilt is due to a combination of biasing of the orientational fluctuations of already tilted molecules and an additional average tilt. The SmA*–C* transition of W107 can thus be said to follow a tilted asymmetric diffuse cone (TADC) model. Both types of X-ray measurements point towards an actual tilt increase of 20°–25°, which means that the ADC model aspect must provide the remaining 20°–25°. Since we of course do not have perfect orientational order in the tilted phase the average molecule tilt in the SmA* phase must be slightly larger than what appears as the ADC contribution to the optical tilt below the phase transition. A reasonable estimate of the average SmA* molecule tilt might thus be 30°. This would give a ‘rod’ length projection factor of $\cos 30^\circ \approx 0.87$ which, with the layer thickness in SmA* measured at 33 Å, gives a rod length of $33/0.87 \approx 38$ Å. This compares well

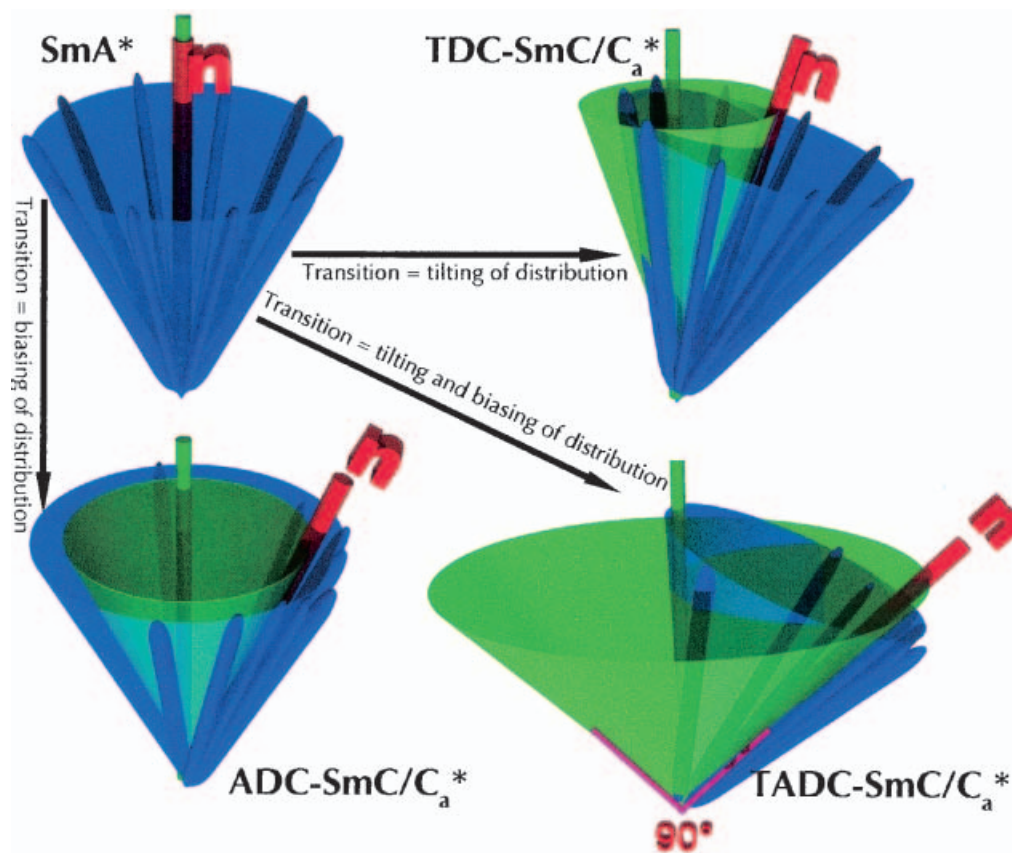


Figure 7. A schematic illustration of three types of diffuse cone model of $\text{SmA}^*-\text{C}^*/\text{C}_a^*$ transitions. In the SmA^* phase (upper, left) the molecular long axes fluctuate uniformly around the layer normal \mathbf{k} (green axis), giving an optical director \mathbf{n} (red axis) parallel to \mathbf{k} . The fluctuations lead to a distribution of molecule orientations over a diffuse cone (blue). The macroscopically observed tilt in SmC^* and SmC_a^* can be generated by the whole distribution cone tilting (upper, right: tilted diffuse cone (TDC) model) or by the distribution being biased towards a certain tilting direction (lower, left: asymmetric diffuse cone (ADC) model). Generally, a combination of these extremes can be expected (lower, right: tilted asymmetric diffuse cone (TADC) model). The green cone is the ordinary $\text{SmC}^*/\text{C}_a^*$ tilt cone, containing the allowed orientations of \mathbf{n} . The TADC model applies to W107, with the TDC and ADC mechanisms both giving strong contributions to the macroscopic properties, producing the unusually large optical tilt with a SmC_a^* tilt cone having an opening angle of 90° .

with the weighted average molecule length in the mixture, 37.1 Å.

As for the origin of the strong ADC model aspect in W107, this is not easy to distinguish. We have mentioned the fact that the mixture contains 33% of molecules that are much longer than the others, and the previous studies of semifluorinated mesogens with ADC transitions [7, 8] suggest that the fluorination of one side chain may play an important role. We may also point out that the change in translational order witnessed at the SmA^*-C^* transition is most likely related to the change in orientational order. In the diffuse cone model SmA^* phase (which is *not* a SmC^* -type phase with random tilt directions, but indeed a SmA^* phase in the sense that the molecules strive for an alignment parallel to \mathbf{k} , but where the thermal disorder produces the diffuse cone of orientations) the molecules fluctuate around \mathbf{k} with quite varying tilt

angles. Even with uniform molecular length these fluctuations must lead to a constant temporal and spatial variation in smectic layer thickness, resulting in reduced effective smectic order and thus reduced X-ray scattering intensity, in particular to higher harmonics. If we in addition introduce a compound with molecules much longer than the rest, the smectic order can only be lowered. On the other hand, in a phase where the molecules strive to tilt away from \mathbf{k} the effect on the smectic order of the 'too long' molecules should not be so large since the fluctuations, which are first of all of smaller magnitude than in SmA^* , are now centered around an orientation not along \mathbf{k} , but with a considerable inclination to that direction.

5. Conclusions

By comparing optical and X-ray investigations of the orthoconic antiferroelectric liquid crystal mixture W107

we conclude that the molecules exhibit a considerable tilt already in the SmA* phase, as predicted by the de Vries diffuse cone model, with uniform orientational fluctuations giving a director parallel to the layer normal. In the SmC* and SmC_a* phases these fluctuations are biased, producing an effective optical tilt as well as a birefringence increase, reflecting the increase in orientational order. In addition, the direction around which the molecules fluctuate tilts away from the layer normal, giving rise to a certain layer shrinkage and a broadening of the wide-angle X-ray scattering pattern. Together these two mechanisms give rise to the unusually high saturation optical tilt of $\theta \approx 45^\circ$ in the SmC_a* phase. In the de Vries terminology, the tilting transition in W107 is thus of a tilted asymmetric diffuse cone model type. The smectic layer boundaries are considerably more well defined in the tilted phases as compared with the SmA* phase, producing a much stronger small angle X-ray scattering with several diffraction orders being detectable in the SmC_a* phase.

We thank J. Springer, TU-Berlin, for provision of the WAXS camera. Financial support from the Deutsche Forschungsgemeinschaft and the Alexander von Humboldt Foundation (J.L.) is gratefully acknowledged.

References

- [1] CHANDANI, A. D. L., HAGIWARA, T., SUZUKI, Y., OUCHI, Y., TAKEZOE, H., and FUKUDA, A., 1988, *Jpn. J. appl. Phys. Lett.*, **27**, L729.
- [2] LAGERWALL, S. T., DAHLGREN, A., JÄGEMALM, P., RUDQUIST, P., D'HAVÉ, K., PAUWELS, H., DABROWSKI, R., and DRZEWINSKI, W., 2001, *Adv. func. Mater.*, **11**, 87.
- [3] D'HAVÉ, K., DAHLGREN, A., RUDQUIST, P., LAGERWALL, J. P. F., ANDERSSON, G., MATUSZCZYK, M., LAGERWALL, S. T., DABROWSKI, R., and DRZEWINSKI, W., 2000, *Ferroelectrics*, **244**, 415.
- [4] D'HAVÉ, K., RUDQUIST, P., LAGERWALL, S. T., PAUWELS, H., DRZEWINSKI, W., and DABROWSKI, R., 2000, *Appl. Phys. Lett.*, **76**, 3528.
- [5] DE VRIES, A., EKACHAI, A., and SPIELBERG, N., 1979, *Mol. Cryst. liq. Cryst. Lett.*, **49**, 143.
- [6] GIESSELMANN, F., ZUGENMAIER, P., DIERKING, I., LAGERWALL, S. T., STEBLER, B., KASPAR, M., HAMPLOVA, V., and GLOGAROVA, M., 1999, *Phys. Rev. E.*, **60**, 598.
- [7] LAGERWALL, J. P. F., GIESSELMANN, F., and RADCLIFFE, M. D., 2002, *Phys. Rev. E*, **66**, 031703.
- [8] GIESSELMANN, F., LAGERWALL, J. P. F., ANDERSSON, G., and RADCLIFFE, M. D., 2002, *Phys. Rev. E*, **66**, 051704.
- [9] GIESSELMANN, F., LANGHOFF, A., and ZUGENMAIER, P., 1997, *Liq. Cryst.*, **23**, 927.
- [10] DRZEWINSKI, W., CZUPRYNSKI, K., DABROWSKI, R., PRZEDMOJSKI, J., NEUBERT, M. E., YAKOVENKO, S. Y., and MURAVSKI, A. A., 2000, *Mol. Cryst. Liq. Cryst.*, **351**, 297.
- [11] RASZEWSKI, Z., KEDZIERSKI, J., RUTKOWSKA, J., PIECEK, W., PERKOWSKI, P., CZUPRYNSKI, K., DABROWSKI, R., DRZEWINSKI, W., ZIELINSKI, J., and ZMIJA, J., 2001, *Mol. Cryst. Liq. Cryst.*, **366**, 607.
- [12] DRZEWINSKI, W., DABROWSKI, R., CZUPRYNSKI, K., PRZEDMOJSKI, J., and NEUBERT, M., 1998, *Ferroelectrics*, **212**, 281.
- [13] DABROWSKI, R., 2000, *Ferroelectrics*, **243**, 1.
- [14] FAFARA, A., GANZKE, D., HAASE, W., MARZEC, M., WROBEL, S., CZAPCZYNSKI, C., and DABROWSKI, R., 2002, *Ferroelectrics*, **276**, 29.
- [15] SAIPA, A., and GIESSELMANN, F., 2002, *Liq. Cryst.*, **29**, 347.
- [16] MIYASATO, K., ABE, S., TAKEZOE, H., and FUKUDA, A., 1983, *Jpn. J. appl. Phys. Lett.*, **22**, L661.
- [17] FAFARA, A., GESTBLOM, B., WROBEL, S., DABROWSKI, R., DRZEWINSKI, W., KILIAN, D., and HAASE, W., 1998, *Ferroelectrics*, **212**, 79.
- [18] HEPPKE, G., LÖTZSCH, D., KAMPA, B., SCHERF, K., and ZASCHKE, H., 1993, *J. prakt. Chem.*, **335**, 549.
- [19] SCHACHT, J., DIERKING, I., GIESSELMANN, F., MOHR, K., ZASCHKE, H., KUCZYNSKI, W., and ZUGENMAIER, P., 1995, *Liq. Cryst.*, **19**, 151.
- [20] MEISTER, R., and STEGEMEYER, H., 1993, *Ber. Bunsenges. Phys. Chem.*, **97**, 1242.
- [21] ZEKS, B., CARLSSON, T., FILIPIC, C., and URBAN, B., 1988, *Ferroelectrics*, **84**, 3.
- [22] DE VRIES, A., 1979, *J. chem. Phys.*, **71**, 25.
- [23] DE VRIES, A., 1979, *Mol. Cryst. Liq. Cryst. Lett.*, **49**, 179.
- [24] DE VRIES, A., 1980, in *Advances in Liquid Crystal Research and Applications*, edited by L. Bata (Oxford, Budapest: Pergamon Press), p. 71.
- [25] TAKANISHI, Y., IKEDA, A., TAKEZOE, H., and FUKUDA, A., 1995, *Phys. Rev. E*, **51**, 400.
- [26] GLASER, M., and CLARK, N., 2002, *Phys. Rev. E.*, **66**, 021711.
- [27] WALBA, D. M., 2003, in *Topics in Stereochemistry, Materials-Chirality*, Vol. 24, edited by M. M. Green, R. J. M. Nolte, E. W. Meijer, and S. E. Denmark (Wiley-VCH), 457.
- [28] BERESNEV, L. A., BLINOV, L. M., OSIPOV, M. A., and PIKIN, S., 1988, *Mol. Cryst. liq. Cryst.*, **158A**, 1.